The Plant Cell, Vol. 27: 2941–2955, October 2015, www.plantcell.org

Arabidopsis TRIGALACTOSYLDIACYLGLYCEROL5 Interacts with TGD1, TGD2, and TGD4 to Facilitate Lipid Transfer from the Endoplasmic Reticulum to Plastids

Jilian Fan, Zhiyang Zhai,[1] Chengshi Yan,[1,2] and Changcheng Xu[3]

Biological, Environmental, and Climate Sciences Department, Brookhaven National Laboratory, Upton, New York 11973

ORCID IDs: 0000-0002-6821-6583 (J.F.); 0000-0003-3181-1773 (Z.Z.); 0000-0002-0179-9462 (C.X.)

The biogenesis of photosynthetic membranes in the plastids of higher plants requires an extensive supply of lipid precursors from the endoplasmic reticulum (ER). Four TRIGALACTOSYLDIACYLGLYCEROL (TGD) proteins (TGD1,2,3,4) have thus far been implicated in this lipid transfer process. While TGD1, TGD2, and TGD3 constitute an ATP binding cassette transporter complex residing in the plastid inner envelope, TGD4 is a transmembrane lipid transfer protein present in the outer envelope. These observations raise questions regarding how lipids transit across the aqueous intermembrane space. Here, we describe the isolation and characterization of a novel *Arabidopsis thaliana* gene, *TGD5*. Disruption of TGD5 results in similar phenotypic effects as previously described in *tgd1,2,3,4* mutants, including deficiency of ER-derived thylakoid lipids, accumulation of oligogalactolipids, and triacylglycerol. Genetic analysis indicates that *TGD4* is epistatic to *TGD5* in ER-to-plastid lipid trafficking, whereas double mutants of a null *tgd5* allele with *tgd1-1* or *tgd2-1* show a synergistic embryo-lethal phenotype. *TGD5* encodes a small glycine-rich protein that is localized in the envelope membranes of chloroplasts. Coimmunoprecipitation assays show that TGD5 physically interacts with TGD1, TGD2, TGD3, and TGD4. Collectively, these results suggest that TGD5 facilitates lipid transfer from the outer to the inner plastid envelope by bridging TGD4 with the TGD1,2,3 transporter complex.

INTRODUCTION

Intracellular lipid transfer is a fundamental aspect of membrane biology and is essential for membrane proliferation, organelle biogenesis, and cell growth. In plants, the endoplasmic reticulum (ER) and the plastid envelope represent the major cellular sites of glycerolipid assembly. These biogenic membranes collaborate in the biosynthesis of the most abundant polar lipids in nature, the thylakoid glycolipids (Browse and Somerville, 1991; Ohlrogge and Browse, 1995), which imposes the need for extensive trafficking of lipids and lipid precursors between, within, and across subcellular membranes. However, the underlying molecular mechanisms of lipid transfer have just begun to emerge from biochemical and genetic analyses, mostly in the model plant *Arabidopsis thaliana* (Benning, 2009).

Both the prokaryotic and eukaryotic pathways contribute to thylakoid lipid assembly from fatty acids synthesized de novo in the plastids in many plants including Arabidopsis. These two pathways differ in the formation of phosphatidic acid (PA) but converge at the generation of diacylglycerol (DAG). The prokaryotic pathway is confined to the plastid, beginning with stepwise acylation of glycerol-3-phosphate to produce PA with a 16-carbon (C16) fatty acid at the *sn-2* position of the glycerol backbone. Dephosphorylation of PA to DAG is catalyzed by PA phosphatase residing in the plastid inner envelope. DAG is a precursor for the synthesis of the major thylakoid glycolipid monogalactosyldiacylglycerol (MGDG) and the sulfolipid sulfoquinovosyldiacylglycerol in the inner envelope membrane (Awai et al., 2001; Benning, 2007). Galactosylation of MGDG generates digalactosyldiacylglycerol (DGDG) at the outer envelope membrane (Dörmann et al., 1999). In the eukaryotic pathway of thylakoid lipid synthesis, fatty acids exported from the plastid are first acylated into phosphatidylcholine (PC) through an acyl editing mechanism (Bates et al., 2007, 2009). Acyl groups released from PC acyl editing are used to synthesize PA and DAG with an 18-carbon (C18) fatty acid attached to the *sn-2* position by acyltransferases and PA phosphatases in the ER, respectively. The resultant DAG is a direct substrate for synthesis of extraplastidic membrane phospholipids including PC. A major proportion of DAG moieties assembled in the ER are returned to the plastid to support thylakoid glycolipid synthesis in envelope membranes (Roughan and Slack, 1982; Browse and Somerville, 1991; Ohlrogge and Browse, 1995). In leaves of Arabidopsis, the contributions of the two pathways to chloroplast lipid synthesis are nearly equal according to the presence of C16 or C18 fatty acids at the *sn-2* position of their DAG backbones. This is in contrast with many other plants, such as pea (*Pisum sativum*) and maize (*Zea mays*), which lack the prokaryotic glycolipid pathway and therefore depend entirely on the import of ER-derived DAG moieties for constructing their own thylakoid membrane lipids (Browse and Somerville, 1991; Ohlrogge and Browse, 1995).

The identity of the lipids imported from the ER to the plastid remains elusive. The proposed candidates include PC (Tanaka et al., 1980), lysophosphatidylcholine (Mongrand et al., 2000; Jessen et al., 2015), or DAG (Williams et al., 2000). In addition,

[1] These authors contributed equally to this work.
[2] Current address: Center for Plant Lipid Research, University of North Texas, Denton, TX 76203.
[3] Address correspondence to cxu@bnl.gov.
The author responsible for distribution of materials integral to the findings presented in this article in accordance with the policy described in the Instructions for Authors (www.plantcell.org) is: Changcheng Xu (cxu@bnl.gov).
www.plantcell.org/cgi/doi/10.1105/tpc.15.00394

detailed characterization of the Arabidopsis *trigalactosyldiacylglycerol* (*tgd*) mutants and functional analyses of the respective TGD proteins implicate PA as the lipid transferred from the ER to chloroplasts for the synthesis of thylakoid glycolipids (Xu et al., 2005; Awai et al., 2006; Wang et al., 2012). To date, four TGD proteins, TGD1,2,3,4, have been identified by genetic approaches (Xu et al., 2003, 2008; Awai et al., 2006; Lu et al., 2007). Disruption of any of the four corresponding genes results in deficiency in eukaryotic thylakoid galactolipids and accumulation of triacylglycerol (TAG) and unusual oligogalactolipids, in particular trigalactosyldiacylglycerol (TGDG) in leaves. Among the four TGD proteins, TGD1, TGD2, and TGD3 are similar to the permease, the substrate binding protein and the ATPase of a bacterial-type ATP binding cassette transporter, respectively. Recent biochemical studies showed that TGD2 interacts with TGD1 and TGD3 in vivo and these three proteins form a stable protein complex of >500 kD localized in the inner envelope membrane of the chloroplast (Roston et al., 2012). TGD4, on the other hand, is an integral membrane protein of the outer chloroplast envelope, and unlike TGD1,2,3 proteins, TGD4 appeared not to stably interact with other proteins but formed a homodimer in vivo (Wang et al., 2012). However, the localization of two physically independent TGD protein complexes in different envelope membranes raises questions as to how lipids transit through the aqueous intermembrane space. Here, we describe the identification and characterization of a novel protein, TGD5. Inactivation of TGD5 results in almost identical lipid phenotypes as *tgd1,2,3,4* mutants. Coimmunoprecipitation analyses showed that TGD5 physically interacts with all of the other four TGD proteins. The possible functions and modes of action of TGD5 in trafficking of lipids from the ER to the plastid are discussed.

RESULTS

Isolation of the *tgd5* Mutant

To identify additional players involved in ER-to-plastid lipid transport, we initiated a forward genetic screen employing a *fatty acid desaturase6* (*fad6*) mutant. The rationale for the screen is based on extensive genetic evidence showing that the *fad6* mutant is dependent on import of polyunsaturated lipid precursors from the ER for thylakoid lipid assembly (Browse et al., 1989), a process involving TGD proteins (Xu et al., 2010). Whereas the *fad6* mutant itself is similar to the wild type in terms of growth and development, the *fad2 fad6* double mutant, which is deficient in the conversion of 18:1 to 18:2 in both the ER and plastids, is chlorotic because polyunsaturated fatty acids that are necessary for a competent photosynthetic membrane system are lacking (McConn and Browse, 1998). Given the crucial role of polyunsaturated fatty acids in chloroplast biogenesis and function (McConn and Browse, 1998), we reasoned that mutants impaired in ER-to-plastid lipid trafficking would be pale green in a *fad6* mutant background due to their deficiency in polyunsaturated fatty acids in the chloroplast.

To test this hypothesis, we mutagenized ~40,000 *fad6* seeds with ethyl methanesulfonate (Xu et al., 2003). M2 plants were grown under continuous light at 22°C. Small leaf samples from individual 3-week-old M2 plants with pale green appearance were used to determine the fatty acid composition by gas-liquid chromatography. From ~25,000 plants screened in this way, we isolated *tgd1,2,3,4* alleles along with M8-16, which also accumulated oligogalactolipids including TGDG in leaves. Genetic complementation testing showed that M8-16 is not allelic to *tgd1-1*, *tgd2-1*, *tgd3-1*, or *tgd4-1* and was thus designated *tgd5-1 fad6*. This mutant was subsequently outcrossed to the wild type. The self-pollinated F1 plants produced F2 populations that segregated for pale-green plants (Supplemental Figure 1A) in a ratio of ~16 to 1 (26 out of 423, 6.15%), and all the 26 pale-green plants accumulated TGDG in leaves and showed an ~2-fold increase in 18:1 and 18:2 with a corresponding decrease in 18:3 in total leaf lipids relative to *fad6* (Supplemental Figure 1B), suggesting that the altered fatty acid composition, the accumulation of TGDG, and the pale-green phenotype are tightly linked and cosegregate as a single recessive trait in the *fad6* background. On the basis of fatty acid profiles of total leaf lipids and the accumulation of TGDG, we were able to identify the homozygous mutant in the wild-type background in the F2 generation, allowing us to investigate the biological consequences of the mutation independently of *fad6*.

The *tgd5-1* Mutation Defines Arabidopsis Gene At1g27695

To identify the mutation responsible for the lipid phenotype, the *tgd5-1* mutant was outcrossed to ecotype Landsberg *erecta* to generate a mapping population that was used for positional cloning of the *tgd5-1* locus. On the basis of oligogalactolipid accumulation, we selected a total of 700 *tgd5-1* mutant plants from the mapping population, and *tgd5-1* was delimited to an ~120-kb region flanked by simple sequence length polymorphism markers T22C5 and F17L21 (Figure 1A). Sequencing of the coding regions for some of the predicted genes of unknown function from the *tgd5-1* mutant identified a G-to-A mutation in the gene At1g27695 (Figure 1B). This mutation results in a Gly-to-Asp substitution in position 41 of the predicted protein. Two independent T-DNA insertion lines (SAIL_254_A11, designated as *tgd5-3*, insertion at nucleotide 639; and SAIL_439_C07, designated as *tgd5-2*, insertion at nucleotide 930 of the genomic sequence; The Arabidopsis Information Resource accession number 4010717885; Figure 1B) were available (Sessions et al., 2002). Analysis of homozygous plants for these two T-DNA mutants revealed the accumulation of oligogalactolipids in leaves (Figure 1C). PCR experiments using cDNA from homozygous mutant plants showed that both T-DNA lines lack the full-length transcript that is present in *tgd5-1* and wild-type plants, but mRNA containing at least the first three of total four exons is present in *tgd5-2* (Figure 1D). These results suggest that *tgd5-2* may be leaky to some extent, while *tgd5-3* is likely a null TGD5 mutant allele.

A full-length wild-type cDNA for At1g27695, which was C-terminally fused to an open reading frame encoding green fluorescent protein (GFP) and driven by the cauliflower mosaic virus (CaMV) 35S promoter, was introduced into the *tgd5-1* homozygous mutant. Expression of the fusion construct in the *tgd5-1* mutant background largely reversed the growth phenotype (Supplemental Figure 2A) and abolished the ability to produce TGDG (Supplemental Figure 2B), consistent with functional complementation of *tgd5-1*. The presence of *tgd5-1* homozygous mutant locus was confirmed by PCR-based genotyping in two

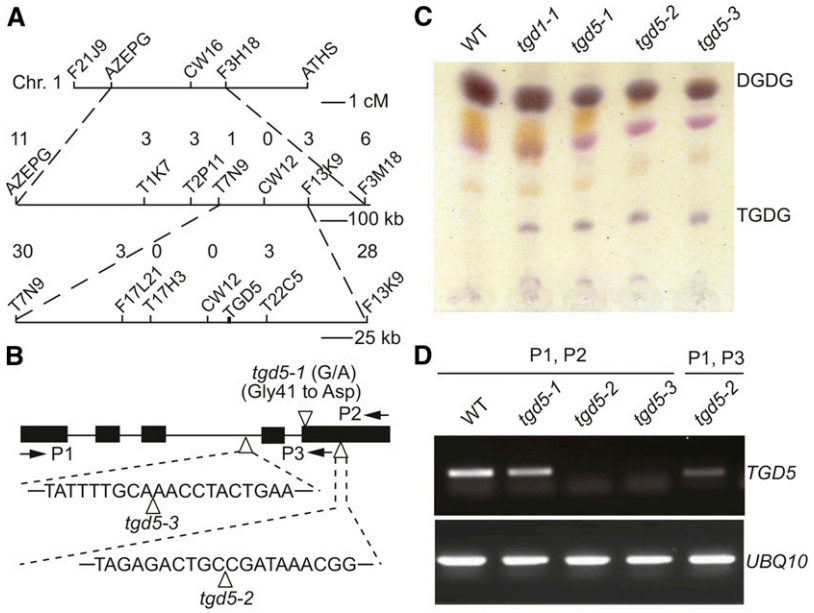

Figure 1. Identification of the *TGD5* Locus.

(A) Map position of the *tgd5-1* mutation on chromosome 1. Markers used for mapping and the respective number of recombinations are indicated.
(B) Structure of *TGD5* (At1g27695). The coding region of At1g27695 is shown as black boxes and introns are indicated by lines. The point mutation in the *tgd5-1* mutant allele is indicated with a triangle, as are the positions of T-DNA insertions in the *tgd5-2* and *tgd5-3* alleles. Arrows indicate the positions of primer pairs used to amplify the *TGD5* transcripts shown in **(D)**.
(C) Lipid phenotype of *tgd5* mutants. A section of thin-layer chromatogram stained for glycolipids is shown.
(D) RT-PCR analysis of *TGD5* expression in wild-type (WT) and *tgd5* plants. Primers (P1, P2, and P3) used for PCR amplification are indicated in **(B)**.

independent transgenic lines (Supplemental Figure 2C). Based on multiple independent lines and complementation analysis, we concluded that At1g27695 is Arabidopsis *TGD5*.

The Phenotype of *tgd5* Mutants Is Similar to, but Less Severe Than, That of *tgd1-1*

The growth and developmental phenotypes of *tgd5* mutants are shown in Figure 2. Similar to *tgd1-1*, all three *tgd5* mutants had a reduced rosette size (Figures 2A and 2D) and were slightly pale in color (Figure 2A). The growth retardation was also apparent at later stages of development in *tgd5-1* and *tgd5-3*, and to a lesser extent also in *tgd5-2* (Figure 2B). In general, the growth reduction was less pronounced in *tgd5* mutants compared with *tgd1-1*. Similar to *tgd1-1*, all three *tgd5* mutants flowered earlier than the wild type (Figure 2E). While visual inspection of developing siliques revealed no obvious difference in seed size and seed setting between the wild type and *tgd5* mutants, quantitative analysis of open mature siliques uncovered small but significant increases in the percentage of aborted seeds in *tgd5-1* and *tgd5-3*, but not in *tgd5-2* (Figure 2F). As a consequence, the germination rate of both *tgd5-1* (91.6% $\pm$ 3.3%) and *tgd5-3* (90.8% $\pm$ 3.1%) seeds was significantly ($P < 0.05$, Student's *t* test) reduced compared with the wild type (98.2% $\pm$ 1.8%), whereas *tgd5-2* (96.6% $\pm$ 2.7%) seeds germinated at a similar frequency to the wild type. About half of seeds were aborted in the *tgd1-1* mutant (Figure 2F), as previously reported (Xu et al., 2005).

Like other *tgd* mutants (Xu et al., 2003; Awai et al., 2006; Lu et al., 2007; Xu et al., 2008), there were substantial increases in 16:0, 18:1, and 18:2 at the expense of 16:3 and 18:3 in leaves of *tgd5* mutants (Figure 3A). Among the three *tgd5* mutant alleles, the changes in leaf fatty acid profiles appeared to be less pronounced in *tgd5-2*, but similar between *tgd5-3* and *tgd5-1*. Polar lipid profiling showed that, similar to findings on the previously characterized *tgd1-1* mutant (Xu et al., 2005), *tgd5* mutants displayed substantially reduced levels of galactolipids with concomitant increases in PC (Figure 3B). It has recently been shown that increased PC promotes flowering via interaction with the Arabidopsis florigen FT (Nakamura et al., 2014). Therefore, it is possible that the early flowering phenotype of *tgd* mutants is due to increases in PC levels.

The fatty acid composition of major membrane lipids was also changed (Supplemental Figure 3). Notably, there were significant increases in 18:1 at the expense of 18:3 in both thylakoid lipids MGDG and DGDG and extraplastidic phospholipids PC and phosphatidylethanolamine. In addition, the relative amounts of C16 fatty acids tended to increase in galactolipids, which resulted in an increase in the ratio of C16 to C18 fatty acids, particularly in DGDG (Figure 4A). Analysis of acyl chain distribution following the position-specific lipase digestion of galactolipids showed that the increase in C16/C18 ratio was associated with a decrease in relative amounts of C18 fatty acids at the *sn-2* position of MGDG and DGDG (Figure 4B), suggesting a compromised eukaryotic pathway of thylakoid lipid synthesis in *tgd5* mutants. Importantly,

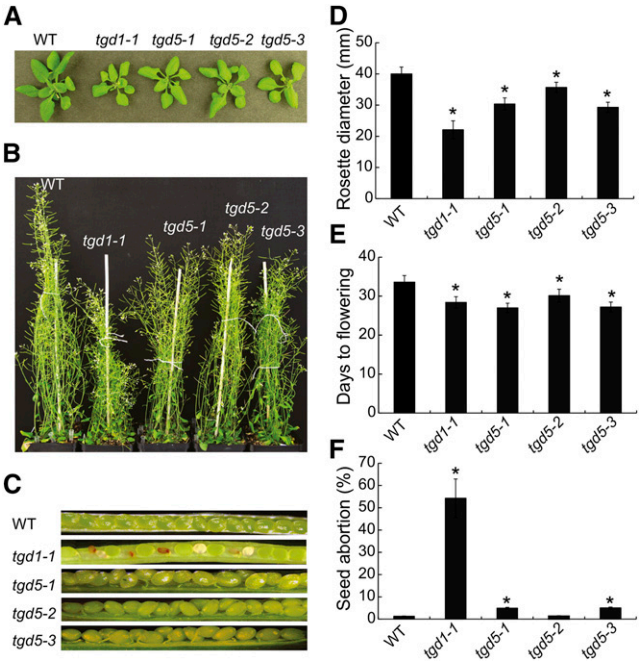

Figure 2. Growth and Developmental Phenotypes of *tgd5* Mutants.

(A) Four-week-old plants grown on agar plates supplemented with 1% sucrose.
(B) Seven-week-old plants grown in soil.
(C) Representative siliques opened up to expose the developing seeds.
(D) Rosette size of 3-week-old plants grown in soil.
(E) Days to flowering in plants grown under a photosynthetic photon flux density of 150 to 200 μmol m^{-2} s^{-1} at 22/18°C (day/night) with a 16-h-light/8-h-dark period.
(F) Percentage of aborted seeds in mature siliques.
Asterisks in **(D)** to **(F)** indicate statistically significant differences from the wild type (WT) based on Student's *t* test ($P < 0.05$). Values are the means and SE of 10 and 15 plants and 10 siliques from five plants in **(D)**, **(E)**, and **(F)**, respectively.

the decrease in relative levels of C18 at the *sn-2* position of galactolipids was much less pronounced in *tgd5-1* and *tgd5-3*, compared with *tgd1-1* (Figures 4B), even though *tgd1-1* carries a leaky point mutation (Xu et al., 2005), whereas *tgd5-3* is a null knockout allele (Figure 1D).

TAG accumulation in leaf tissues is a lipid phenotype shared by all known *tgd* mutants (Xu et al., 2005, 2008; Awai et al., 2006; Lu et al., 2007). Analysis of leaf lipid extracts of *tgd5-1*, *tgd5-2*, and *tgd5-3* mutants by thin-layer chromatography (TLC) revealed an accumulation of neutral lipids comigrating with TAGs present in the *tgd1-1* mutant as well (Figure 5A). In addition, the ultrastructure of *tgd5-1* leaf mesophyll cells revealed the presence of lipid droplets in the cytosol (Figure 5B), similar to what was reported for *tgd1-1* (Xu et al., 2005) and *tgd4* (Xu et al., 2008). Quantification of neutral lipids in leaves of 4-week-old plants grown in soil showed that TAG levels increased by ~11-fold in *tgd1-1*, *tgd5-1*, and *tgd5-3*, but only by 3-fold in *tgd5-2*, compared with the wild type (Figure 5C).

The increased TAG accumulation in *tgd1-1* has been attributed, at least partially, to enhanced fatty acid synthesis in leaves (Fan et al., 2013a, 2013b). To test whether fatty acid metabolism is also affected in *tgd5* mutants, we performed in vivo pulse-chase labeling experiments with ^{14}C-acetate. We detected 4.9-, 3-, 1.8-, and 2.6-fold increases in the rate of label incorporation into total lipids in growing leaves of 5-week-old *tgd1-1*, *tgd5-1*, *tgd5-2*, and *tgd5-3* mutant plants, respectively, compared with the wild type (Figure 6A). During the 3-d chase period, the label decreased by 15% in the wild type, 71% in *tgd1-1*, and 36 to 51% in *tgd5* mutants (Figure 6B). These results suggest that disruption of the eukaryotic thylakoid lipid pathway results in increases in the rates of both synthesis and turnover of fatty acids in *tgd5* mutants, similar to the situation found for *tgd1-1* (Fan et al., 2013a).

We recently demonstrated that TAG is a key intermediate in fatty acid turnover in leaves of *tgd1-1* (Fan et al., 2014). To determine whether this is also the case in *tgd5* mutants, we generated a double mutant between *tgd5-3* and *sdp1-4*, a T-DNA insertion mutant disrupted in SUGAR-DEPENDENT1 (SDP1) TAG lipase responsible for initiating TAG breakdown during early seedling establishment (Eastmond, 2006). Microscopy examination of mature leaves stained with the neutral lipid-specific dye, Nile red, revealed a drastic increase in the size of lipid droplets in the *tgd5-3 sdp1-4* double mutant, compared with either parent (Figure 7). Quantification of leaf lipid extracts from 7-week-old soil-grown plants showed that the amounts of leaf TAG increased to 8.0% per dry weight in the double mutant, a 114- and 6.7-fold increase compared with the wild type and *tgd5-3*, respectively (Figure 7E). The increase in TAG content was accompanied by a corresponding increase in total leaf fatty acid content in the double

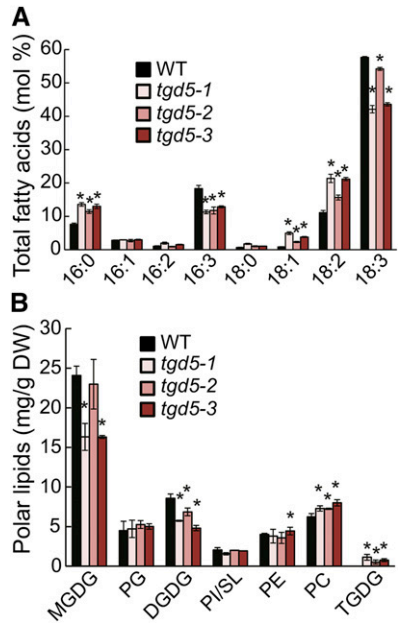

Figure 3. Lipid Phenotypes of *tgd5* Mutants.

Lipids were extracted from 4-week-old plants grown in soil. Values are means of three replicates with SE. Asterisks indicate statistically significant differences from the wild type (WT) based on Student's *t* test ($P < 0.05$).
(A) Total leaf fatty acid composition.
(B) Leaf membrane lipid composition. PE, phosphatidylethanolamine; PG, phosphatidylglycerol; PI, phosphatidylinositol; SL, sulfoquinovosyldiacylglycerol.

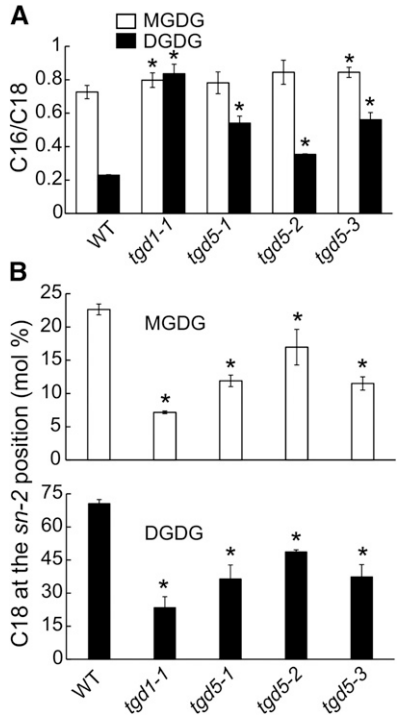

Figure 4. Compositional and Positional Analyses of Galactolipid Acyl Groups of *tgd5* Mutants.

(A) Ratios of C16 versus C18 fatty acids in galactolipids from leaves of wild-type (WT), *tgd1-1*, and *tgd5* mutant plants. C16 indicates the sum of 16: 0, 16: l, 16:2, and 16:3; C18 indicates the sum of 18:0, 18:1, 18:2, and 18:3.
(B) Fatty acid composition exclusively at the *sn-2* position of the glycerol backbone of galactolipids from leaves of wild-type, *tgd1-1*, and *tgd5* mutant plants.
Data are the means of three replicates with SE. Asterisks indicate statistically significant differences from the wild type based on Student's *t* test ($P < 0.05$).

mutant (Figure 7F), suggesting that TAG accumulation is due to decreased fatty acid turnover rather than a net conversion of membrane lipids to TAG. These results lend further support for a critical role for TAG metabolism in fatty acid turnover in leaves. Fatty acid compositional analysis showed that the predominant acyl chains in leaf TAG in *tgd1-1* and *tgd5* single and *tgd5-3 sdp1-4* double mutants were 18:2 and 18:3 (Supplemental Figure 4).

The *ats1-1 tgd5* Double Mutants Show Severe Growth and Developmental Defects

To provide genetic evidence that TGD5 is involved in ER-to-plastid lipid trafficking, two different *tgd5* alleles were introduced into the *ats1-1* mutant background by genetic crossing. The *ats1-1* mutant is almost completely blocked in the prokaryotic pathway of thylakoid galactolipid synthesis due to a genetic defect in the plastidic acyl-CoA:glycerol-3-phosphate acyltransferase (Kunst et al., 1988; Xu et al., 2006). Thus, if TGD5 is important for the eukaryotic thylakoid lipid pathway, the combined disruption of both thylakoid lipid biosynthetic pathways in double mutants between *tgd5* and *ats1-1* would be expected to be nonviable or severely impaired in thylakoid membrane biogenesis as previously shown for *ats1-1 tgd1-1* (Xu et al., 2005) and *ats1-1 tgd4* (Xu et al., 2008) double mutants. Indeed, no homozygous *ats1-1 tgd5-1* double mutants were obtained in a large number of F2 progeny plants derived from a cross between the allele *tgd5-1* and the *ats1-1* mutant. In addition, in 62 plants homozygous for *tgd5-1*, only two heterozygous *ats1-1* plants (3.2%) were recovered by diagnostic PCR. This frequency was far below the 50% expected. Furthermore, heterozygous *ats1-1* mutants in the *tgd5-1* background showed stunted growth (Figure 8A), and their siliques (Figure 8B) contained a large fraction (67.5%, 255 out of 378 total seeds) of aborted seeds. When embryos of normal green (Figure 8C) and aborted (Figure 8D) seeds from the same siliques were examined under a microscope, many aborted seeds were found arrested at the heart stage (Figure 8D). Together, these results suggest that the combined mutations in ATS1 and TGD5 are lethal during embryogenesis.

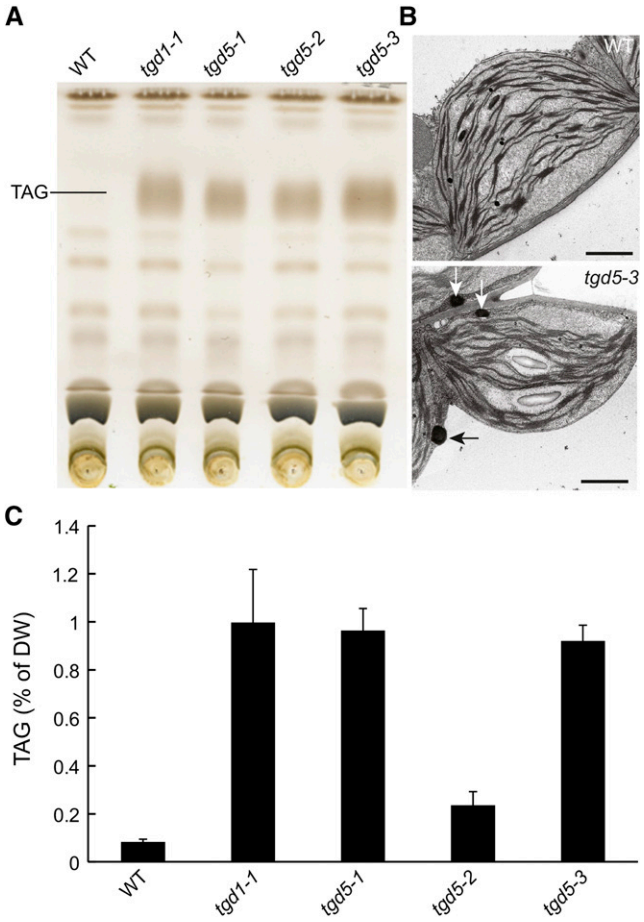

Figure 5. TAG Accumulation in Leaves of *tgd5* Mutants.

(A) Thin-layer chromatogram of neutral lipids. Lipids were isolated from 4-week-old plants and visualized with 5% sulfuric acid by charring.
(B) Transmission electron microscopy images of leaf cells of the wild type (WT) and *tgd5-3*. Arrows indicate lipid droplets. In total, 0 out of 21 and 6 out of 42 cells analyzed for the wild type and *tgd5-3*, respectively, were found to possess at least one oil droplet. Bars = 1 μm.
(C) TAG content in leaves of *tgd5* mutants in comparison with the wild type and *tgd1-1*. Data are the means and SE of four replicates.

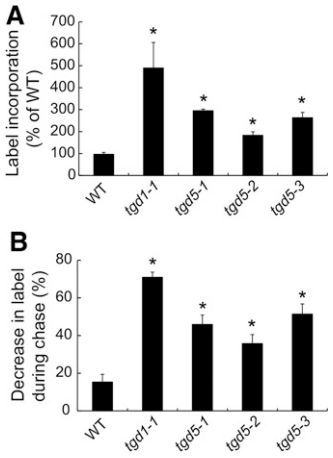

Figure 6. Increases in Rates of Fatty Acid Synthesis and Turnover in Leaves of *tgd5* Mutants.

Six detached developing leaves of 5-week-old plants were labeled with ^{14}C-acetate for 1 h (pulse). After washing three times with water, the leaves were then incubated in unlabeled solution for 3 d (chase). Data are the means and SE of three replicates. Asterisks indicate statistically significant differences from the wild type (WT) based on Student's *t* test ($P < 0.05$). The experiments were repeated three times with similar results.
(A) Label incorporation into total lipids during the pulse.
(B) Decreases in total labeled fatty acids during the chase period.

When the partially impaired *tgd5-2* was crossed with the *ats1-1* mutant, individuals that were homozygous for both mutant alleles could be identified in the F2 population by PCR-based genotyping. Compared with the single mutants, the *ats1-1 tgd5-2* double mutant was severely stunted in growth and pale green in color (Figure 9A). Analysis of major membrane lipids revealed an ~50% reduction in MGDG content with a concomitant increase in phospholipids, particularly PC in the *ats1-1 tgd5-2* double mutant compared with the wild type (Figure 9B). The residual galactolipids in the double mutant contained almost exclusively C18 fatty acids (Figure 9C), suggesting their biosynthetic origin from the eukaryotic pathway due to the presence of the leaky *tgd5-2* allele. Ultrastructural analysis showed that the thylakoid membrane system in chloroplasts of the double mutant was underdeveloped (Figures 9E and 9F). In addition, leaf mesophyll cells of the *tgd5-2 ats1-1* mutant contained only one (Figure 9E) or two (Figure 9F) chloroplast(s), suggesting a block in chloroplast division in the *ats1-1 tgd5-2* double mutant. The chloroplast division defect was also observed in the *ats1-1 tgd4-1* double mutant (Xu et al., 2008), in a T-DNA insertion mutant impaired in fatty acid synthesis (Wu and Xue, 2010), and in double mutants between *fad6* and *tgd1-1* or *tgd4-3* (Fan and Xu, 2011) and is likely due to a shortage of lipid supply for membrane proliferation during chloroplast division (Wu and Xue, 2010).

Genetic Interactions between *TGD5* and Other *TGD* Genes

To test potential genetic interactions between TGD5 and other TGD proteins, we crossed *tgd5-3* with *tgd1-1* (Xu et al., 2005), *tgd2-1* (Awai et al., 2006; Roston et al., 2011), or *tgd4-3* (Xu et al., 2008). In preliminary experiments, we failed to obtain *tgd1-1 tgd5-3* and *tgd2-1 tgd5-3* double mutants in ~200 F2 progeny seedlings for each mutant combination. In the progenies of F2 plants homozygous for *tgd5-3* and heterozygous for *tgd1-1* or *tgd2-1*, again no homozygous *tgd1-1 tgd5-3* and *tgd2-1 tgd5-3* double mutants and only seven and four heterozygous *tgd1-1* (15.2%) and *tgd2-1* (7.7%) mutants were found among 46 and 52 plants tested by PCR for the *tgd1-1* or *tgd2-1* locus, respectively. These segregation values were far below the expected frequency of 50%, suggesting partial embryo lethality in *TGD1/tgd1-1* and *TGD2/tgd2-1* allele combinations in the *tgd5-3* background. Consistent with this, a large portion of seeds were aborted in the heterozygous *tgd1-1* (62.1%, 221 out of 356 total seeds) or heterozygous *tgd2-1* (66.6%, 265/398 total seeds) in the homozygous *tgd5-3* background (Figure 10A). Together, these results suggest that disruption of TGD1 or TGD2 causes embryonic lethality in the *tgd5-3* mutant.

In contrast to the allele combinations between *tgd5-3* and *tgd1-1* or *tgd2-1*, the *tgd4-3 tgd5-3* double mutant was viable, showed a similar growth phenotype to *tgd4-3* (Figures 10B and 10C) and was

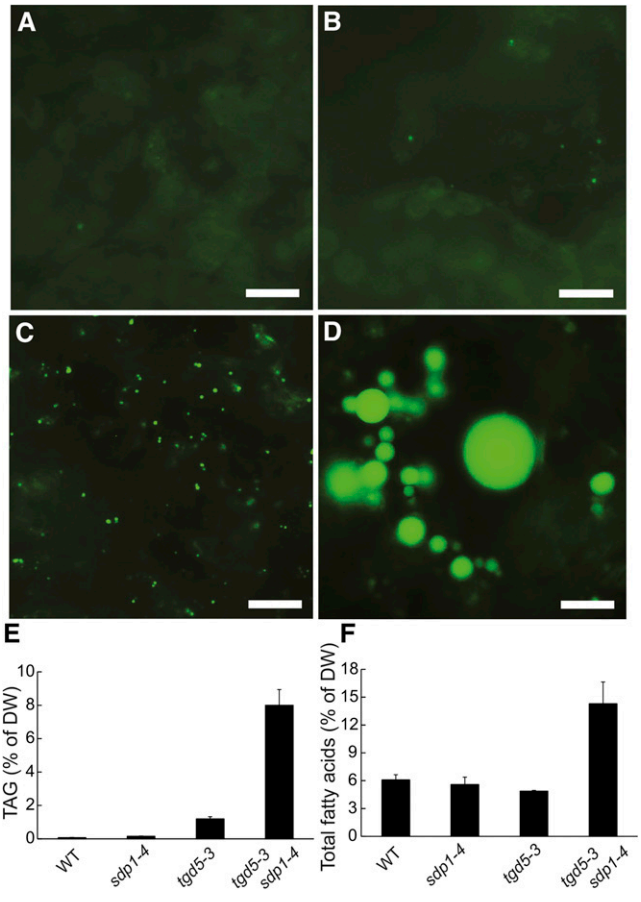

Figure 7. Disruption of SDP1 Enhances Lipid Droplet Accumulation in *tgd5-3* Leaves.

(A) to **(D)** Images of LDs in wild-type **(A)**, *sdp1-4* **(B)**, *tgd5-3* **(C)**, and *tgd5-3 sdp1-4* **(D)** leaf tissues stained with Nile red. Bars = 10 μm.
(E) and **(F)** TAG **(E)** and total fatty acid **(F)** content in leaves of wild-type (WT), *sdp1-4*, *tgd5-3*, and *tgd5-3 sdp1-4* mutant plants. Data are the means and SE of three replicates.

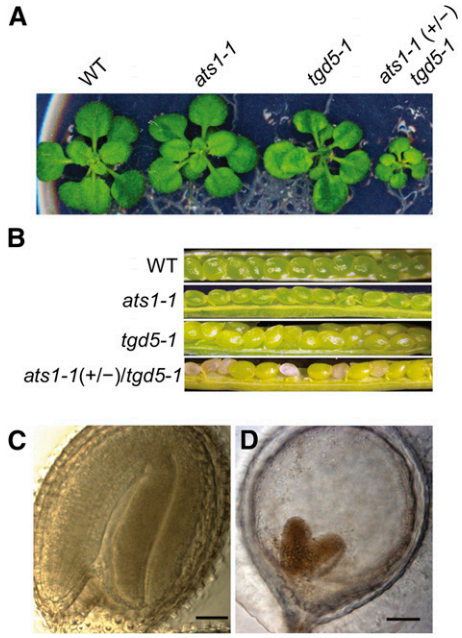

Figure 8. Embryo Lethality of an *ats1-1 tgd5-1* Double Mutant.

(A) Growth phenotype of plants determined to be homozygous for *tgd5-1* and heterozygous for *ats1-1* [*ats1-1*(+/−)] in comparison to the parent lines and the wild type (WT). The plants were grown for 3 weeks on agar-solidified MS medium.

(B) Representative siliques opened up to expose the developing seeds. Wild-type plants and the homozygous *tgd5-1* mutant show full seed set, while more than half of seeds are aborted in *ats1-1*(+/−) *tgd5-1* plants.

(C) and **(D)** Cleared developing seeds from the same silique of *ats1-1*(+/−) *tgd5-1*. Normal seed with a typical mature embryo **(C)** and aborted seed with the embryo arrested at the heart stage **(D)** are shown. Bars = 80 μm.

completely infertile. Viable seeds were obtained when *tgd4-3 tgd5-3* pistils were pollinated with wild-type pollen, but reciprocal pollination did not yield seeds, suggesting that the *tgd4-3 tgd5-3* double mutant is male sterile, similar to what was observed in the *tgd4-3* single mutant (Xu et al., 2008). Assaying pollen viability by Alexander staining indicated that the mature anthers of the *tgd5-3* single and *tgd4-3 tgd5-3* double mutants did contain viable pollen grains (Supplemental Figure 5A). In addition, close examination of the flowers revealed no obvious morphological differences between the wild type and *tgd4-3 tgd5-3* (Supplemental Figure 5B). However, no pollen grains from freshly anther-dehisced flowers of the *tgd4-3 tgd5-3* double mutant germinated in in vivo germination assays (Supplemental Figure 6C), suggesting that the pollen grain germination defect is likely to be the cause for the male sterile phenotype in the double mutant. When grown in soil, the *tgd4-3 tgd5-3* double mutant displayed similar rosette size (Figure 10B), plant height (Figure 10C), polar lipid content (Figure 10D), and fatty acid composition (Supplemental Figure 6) to the *tgd4-3* single mutant. Analysis of fatty acid positional distribution in galactolipids showed that the relative amounts of C18 fatty acids at the *sn-2* position of MGDG and DGDG were similar between *tgd4-3 tgd5-3* and *tgd4-3*, but significantly different between *tgd4-3 tgd5-3* and *tgd5-3* (Figure 10E). These results suggest that TGD4 is epistatic to TGD5 in plant growth and development as well as in the pathway of ER-to-plastid lipid trafficking.

TGD5 Is Localized in the Envelope of Chloroplasts

The *TGD5* gene encodes a small glycine-rich (27.5% glycine) protein with a calculated molecular mass of 9174 D. This protein is predicted to have two membrane spanning domains according to the suite of prediction programs used by the Aramemnon database (http://aramemnon.uni-koeln.de/) (Supplemental Figure 7). A BLAST-based sequence homology search using Arabidopsis TGD5 identified homologous sequences in many higher plants, including rice (*Oryza sativa*), maize, soybean (*Glycine max*), oilseed rape (*Brassica napus*), and tomato (*Solanum lycopersicum*), but no obvious homologs were found in lower plant or nonplant genomes. Thus, TGD5 is likely specific to seed-bearing plants. Interestingly, the Gly-41 residue that is mutated in the *tgd5-1* allele (G41D) is entirely conserved among TGD5 homologs in a region containing the highest degree of similarity (Supplemental Figure 7).

The TGD5 protein does not contain an obvious N-terminal chloroplast transit peptide and is not predicted to be targeted to chloroplasts by the set of subcellular prediction programs used by

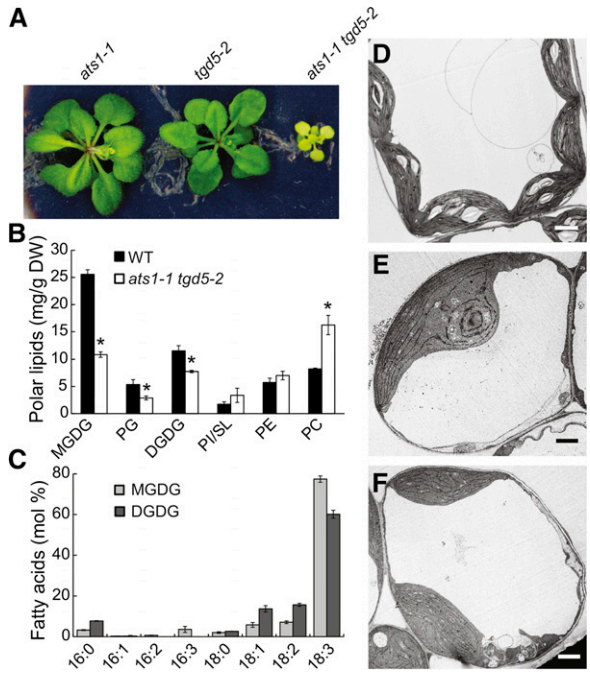

Figure 9. Analysis of the *ats1-1 tgd5-2* Double Homozygous Mutant.

(A) Growth phenotype of the *ats1-1 tgd5-2* double mutant in comparison to the parent lines. The plants were grown for 4 weeks on agar-solidified MS medium.

(B) Leaf lipid composition of wild-type (WT) and *ats1-1 tgd5-2* plants. Data are the means of the three replicates with SE. Asterisks indicate statistically significant differences from the wild type based on Student's *t* test ($P < 0.05$).

(C) Fatty acid composition of leaf galactolipids from wild-type and *ats1-1 tgd5-2* plants. Data are the means of three replicates with SE.

(D) to **(F)** Ultrastructure of leaf cells of the wild type **(D)** and the *ats1-1 tgd5-2* double mutant containing one **(E)** or two **(F)** chloroplasts. Bars = 2 μm.

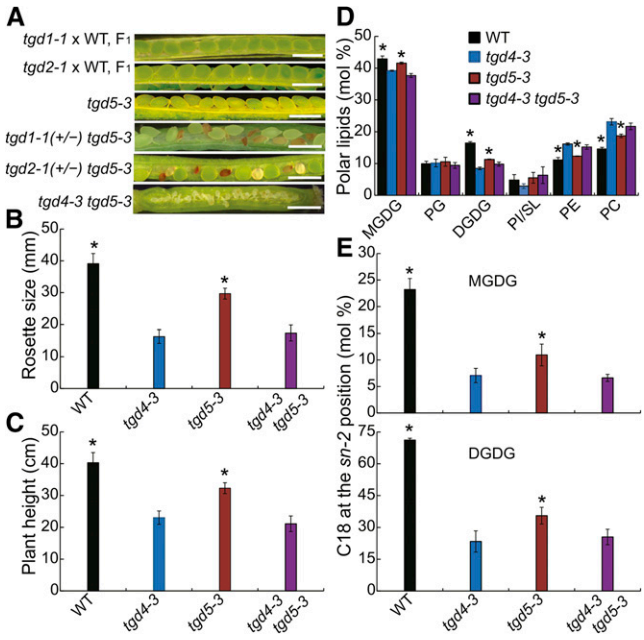

Figure 10. Epistatic Analysis of TGD5 with TGD1, TGD2, and TGD4.

(A) Representative siliques from the *tgd5-3* single or *tgd4-3 tgd5-3* double mutants, from plants heterozygous for *tgd1-1* or *tgd2-1* in the wild-type (WT) background or from plants heterozygous for *tgd1-1* or *tgd2-1* in the homozygous *tgd5-3* mutant background [*tgd1-1*(+/−) *tgd5-3* or *tgd2-1* (+/−) *tgd5-3*]. Bars = 1 mm.
(B) Rosette size of 4-week-old plants grown in soil.
(C) Plant height measured as the length of main inflorescence stalks of 7-week-old plants.
(D) Polar lipid composition in leaves of 4-week-old plants grown in soil.
(E) C18 fatty acid composition exclusively at the *sn-2* position of the glycerol backbone of galactolipids from leaves of single and double mutant plants.
Asterisks in **(B)** to **(E)** indicate statistically significant differences from *tgd4-3* based on Student's *t* test ($P < 0.05$). Values are the means and SE of 15 to 20 plants in **(B)** and **(C)** and three replicates in **(D)** and **(E)**, respectively.

the Arabidopsis subcellular database (Heazlewood et al., 2007). We employed confocal laser microscopy to examine the subcellular localization of TGD5-GFP in stably transformed transgenic lines shown in Supplemental Figure 2A. The fluorescent signals of TGD5-GFP were strictly observed at the peripheral region of chloroplasts (Figure 11A), suggesting a chloroplast envelope localization of TGD5. Subfractionation experiments showed that TGD5-GFP was absent from thylakoids, but highly enriched in envelope membranes of chloroplasts (Figure 11B). To further explore the association of TGD5 with one of the two chloroplast envelope membranes, we employed in vivo chloroplast import and protease protection assays (Xu et al., 2005). For this purpose, TGD5-GFP; four envelope-targeted control proteins, TGD1-HA, TGD2-HA, HA-TGD4 (Xu et al., 2005; Awai et al., 2006; Wang et al., 2012), and OEP7-GFP (Schleiff et al., 2001); and one stromal protein, ATS1-HA (Xu et al., 2005), were transiently expressed in tobacco (*Nicotiana tabacum*) leaves via *Agrobacterium tumefaciens* infection. Intact chloroplasts isolated from leaves expressing the transgenes were then treated with thermolysin, which is unable to penetrate the outer envelope or trypsin, which is able to penetrate the outer but not the inner membrane. In these assays, the TGD5-GFP fusion protein behaved like the inner envelope localized control proteins TGD1 and TGD2 (Awai et al., 2006) and the stromal protein ATS1, being resistant to both thermolysin and trypsin (Figure 11C). As expected, TGD4 and OEP7, proteins associated with the outer envelope of chloroplasts (Schleiff et al., 2001; Wang et al., 2012), were sensitive to both protease treatments (Figure 11C).

TGD5 Physically Interacts with TGD1, TGD2, TGD3, and TGD4

To determine whether TGD5 physically interacts with other TGD proteins, we performed coimmunoprecipitation (Co-IP) assays. To do this, the TGD5-GFP construct driven by the 35S CaMV promoter was coinfiltrated into tobacco leaves with a construct expressing TGD1-HA, TGD2-HA, TGD3-HA, or HA-TGD4. Co-expression of TGD5-GFP with the N-terminal half of an outer envelope membrane protein DGD1 (Froehlich et al., 2001) fused to a HA tag (DGD1N-HA) was used as a negative control. Expression of GFP and HA fusion proteins was verified by immunoblot analysis (Figure 12, input). To test for protein-protein interactions, intact chloroplasts isolated from the infiltrated leaves coexpressing the epitope-tagged fusion proteins were solubilized with dodecylmaltoside. Solubilized chloroplasts were then incubated with agarose beads conjugated with anti-HA antibody and

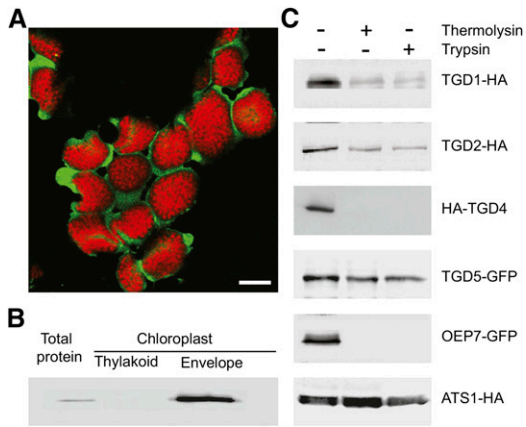

Figure 11. Subcellular Localization of TGD5.

(A) Confocal fluorescence microscopy image of mesophyll cells of 4-week-old plants stably expressing a TGD5-GFP fusion construct. The green fluorescence is indicative of the presence of the TGD5-GFP fusion protein and red fluorescence corresponds to chloroplasts. Bar = 5 μm.
(B) Immunoblot analysis of TGD5 subcellular localization. Total proteins were extracted from leaves of 4-week-old plants overexpressing TGD5-GFP. Chloroplasts isolated from 4-week-old transgenic plants were fractionated into thylakoids and envelopes. Equal amounts of proteins were subjected to immunoblot analysis using an antibody against GFP.
(C) Protease protection assay of TGD5-GFP. The TGD5-GFP, TGD1-HA, TGD2-HA, and HA-TGD4 along with the outer envelope protein OEP7 and the stromal protein ATS1were transiently expressed in tobacco leaves. Chloroplasts were isolated and treated either with thermolysin or trypsin as indicated. Protein gel blots detecting the GFP- and HA-tagged fusion proteins using GFP- or HA-specific antibodies, respectively, are shown.

proteins pulled down by agarose beads were analyzed by immunodetection using antibodies against GFP and HA. As shown in Figure 12, TGD5-GFP proteins were efficiently precipitated by TGD1-HA, TGD2-HA, TGD3-HA, or HA-TGD4. No signal for TGD5-GFP was detected in immunoprecipitates from tobacco leaves coexpressing TGD5-GFP and DGD1N-HA (Figure 12), although both fusion proteins were present in input fractions, thus demonstrating a specific coprecipitation of TGD5 with TGD1, TGD2, TGD3, or TGD4.

DISCUSSION

TGD5 Bridges TGD4 and the TGD1,2,3 Transport Complex in ER-to-Plastid Lipid Trafficking

This study identifies TGD5 as a novel protein component involved in ER-to-plastid lipid trafficking as part of the eukaryotic pathway of thylakoid lipid assembly. Based on available biochemical and genetic evidence, we propose that TGD5 functions in concert with TGD1, TGD2, TGD3, and TGD 4 to shuttle lipid precursors from the ER through the outer chloroplast envelope and the intermembrane space to the stromal side of the inner envelope membrane. In this pathway, TGD5 facilitates lipid transfer across the aqueous intermembrane space by bridging the outer envelope membrane protein TGD4 with the inner envelope TGD1,2,3 transport complex to form a lipid transport supercomplex via direct physical interactions (Figure 13). The energy required to convey ER-derived lipid molecules in discrete steps across the proposed lipid conduit is presumably provided by TGD3-mediated ATP hydrolysis in the stroma of chloroplasts (Lu et al., 2007). The overall structure of the TGD supercomplex is similar to that of the *trans*-envelope lipopolysaccharide transport machinery (Sperandeo et al., 2008; Chng et al., 2010) and the orthologous TGD phospholipid transport pathway (Malinverni and Silhavy, 2009) in *Escherichia coli*. In both of these bacterial lipid transport systems, there is at least one protein component in each cellular compartment, namely, the cytoplasm, the inner envelope, the intermembrane space, and the outer envelope. Disruption of any of the components in the bacterial TGD phospholipid pathway (Sperandeo et al., 2008) or the lipopolysaccharide transport system (Malinverni and Silhavy, 2009) blocks the entire transport process and often leads to similar phenotypes among the mutants lacking individual transport components. Other examples of the transport complexes with their protein components located in two different membranes are the bacterial efflux pumps (Symmons et al., 2009) and the TOC/TIC (Translocon at the Outer/Inner envelope membrane of Chloroplasts) protein import apparatus in chloroplasts of plants (Paila et al., 2015). In the latter case, Tic22, an intermembrane protein of chloroplasts, has been suggested to play a role in bridging TIC and TOC complexes to facilitate protein import across the two chloroplast envelope membranes (Soll and Schleiff, 2004), hence functioning in the same manner as TGD5 in ER-to-plastid lipid trafficking.

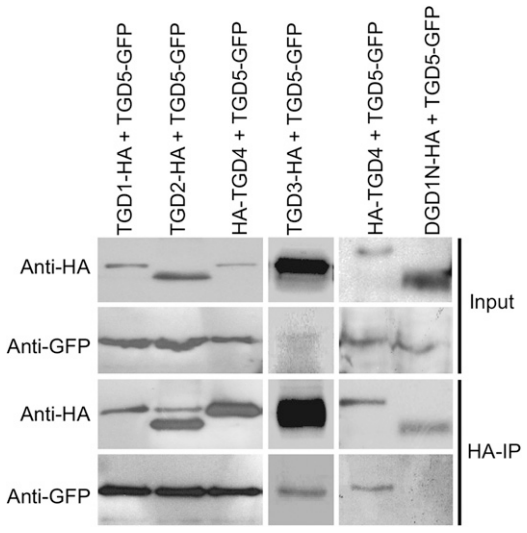

Figure 12. TGD5 Physically Interacts with TGD1, TGD2, TGD3, and TGD4 in Vivo.

TGD5-GFP was transiently coexpressed with TGD1-HA, TGD2-HA, TGD3-HA, HA-TGD4, or DGD1N-HA in tobacco leaves. Solubilized chloroplasts isolated from the infiltrated leaves were immunoprecipitated with anti-HA agarose beads (HA-IP). Total protein extracts (Input) and the HA-agarose-retained proteins were analyzed by immunoblotting using antibodies against HA (anti-HA) or against GFP (anti-GFP).

That five TGD proteins cooperate in shuttling ER-derived lipid precursors across two chloroplast envelope membranes for thylakoid lipid assembly is supported by multiple lines of physiological, biochemical, and genetic evidence. First, disruption of TGD5 results in similar phenotypic changes as found in other *tgd* mutants (Awai et al., 2006; Lu et al., 2007; Xu et al., 2008; Fan et al., 2013a), including deficiency in galactolipids assembled from ER-derived DAG moieties, increases in fatty acid synthesis and turnover, accumulation of oligogalactolipids and TAG, and decreases in vegetative growth. Second, analysis of the *tgd5-1 ats1-1* double mutant provided genetic evidence consistent with a block in the eukaryotic pathway of thylakoid lipid synthesis in *tgd5-1* and the prokaryotic pathway in *ats1-1*. Disrupting both pathways blocks thylakoid lipid synthesis, resulting in embryo lethality as previously shown for *tgd1-1 ats1-1* and *tgd4-3 ats1-1* mutants (Xu et al., 2005, 2008). Third, results from the double mutant analysis showed that *tgd4-3* is epistatic to *tgd5-3* with respect to plant growth and the eukaryotic pathway of galactolipid synthesis. Because both *tgd4-3* (Xu et al., 2008) and *tgd5-3* are null T-DNA knockout mutants, this epistatic genetic interaction is consistent with the involvement of TGD5 in the same lipid trafficking pathway as TGD4, with TGD5 functioning downstream of TGD4. In addition, introducing *tgd5-3* into *tgd1-1* or *tgd2-1* caused an additive embryo-lethal phenotype, suggesting that TGD5 functions in the same pathway as TGD1 and TGD2 and that TGD5 plays an overlapping and partially independent role compared with TGD1 and TGD2 in shuttling ER-derived lipid precursors from the outer to the inner envelope membrane of chloroplasts. Fourth, the results of GFP fusion and chloroplast subfractionation experiments showed that TGD5 is specifically associated with chloroplast envelope membranes, similar to TGD1 and TGD2 (Xu et al., 2005; Awai et al., 2006).

It should be noted that, compared with *tgd1*, *2*, and *4* mutants, null *tgd5* mutants displayed less pronounced reductions in the proportion of galactolipids made by the eukaryotic pathway. This

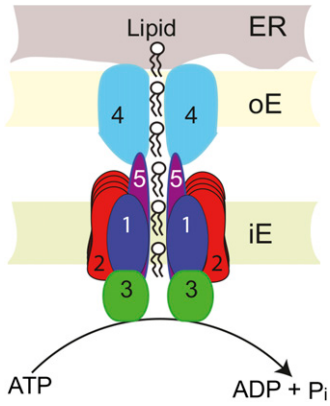

Figure 13. Model for ER-to-Plastid Lipid Trafficking Mediated by TGD Proteins.

In this model, the TGD machinery shuttles lipid precursors from the ER through the outer envelope and the intermembrane space to the stromal side of the inner envelope membrane of chloroplasts. TGD5 facilitates the lipid transfer by bridging TGD4 in the outer envelope with the TGD1, TGD 2, and TGD 3 transport complex in the inner envelope via protein-protein interactions. The model also proposes that part of the TGD4 protein is physically present at ER-chloroplast membrane contact sites, playing a role in the transfer of lipids from the ER to the outer chloroplast envelope (Wang et al., 2012), and the energy required to convey ER-derived lipid molecules across the proposed lipid conduit is presumably provided by TGD3-mediated ATP hydrolysis inside the chloroplast (Lu et al., 2007). Numbers correspond to TGD1, TGD2, TGD3, TGD4, and TGD5 proteins. The dimeric composition is shown for TGD1, TGD3, TGD4, and TGD5 and octameric for TGD2 (Roston et al., 2012). ER, outer (oE), and inner (iE) chloroplast envelope membranes are indicated.

presumably reflects that other routes such as the direct transfer of ER-derived lipid precursors from TGD4 to TGD2 (Roston et al., 2011; Wang et al., 2012; Hurlock et al., 2014), spontaneous movement of lipids between membranes (Lev, 2010) and lipid transfer by hemifused interfaces between the inner leaflet of the outer envelope and the outer leaflet of the inner envelope of chloroplasts (Mehrshahi et al., 2013) may contribute to the eukaryotic pathway of thylakoid biosynthesis. Although the exact contribution of each of these alternative routes to lipid movement across the intermembrane space of chloroplast envelopes remains to be determined, the finding that the double mutants between *tgd5-3* and *tgd1-1* or *tgd2-1* are embryo-lethal may suggest that the direct lipid transfer from TGD4 to TGD2 (Roston et al., 2011; Wang et al., 2012) may account for the majority of the residual ER-to-plastid lipid trafficking activity in the *tgd5* null mutant.

Recent studies suggest that intermembrane lipid transport can be greatly enhanced at membrane contact sites (MCSs), regions where two cellular membranes come into close contact (Lev, 2010; Elbaz and Schuldiner, 2011). MCSs are structured in durable or transient states by molecular tethering factors. Recent biochemical and genetic studies in yeast and mammalian systems have begun to reveal the structural and functional components involved in establishing MCSs (Elbaz and Schuldiner, 2011; Helle et al., 2013; Tatsuta et al., 2014). In plants, the existence of MCSs between the outer and inner chloroplast envelope membranes has long been known based on ultrastructural observations (Carde et al., 1982; Cremers et al., 1988). It remains unclear, however, whether TGD5 is involved in establishing such MCSs by bridging the outer envelope lipid transport protein TGD4 with the TGD1,2,3 transporter of the inner envelope and whether the TGD supercomplex is part of MCSs between the two envelope membranes of chloroplasts.

TGD5 encodes a small protein predicted to harbor two transmembrane-spanning domains that are highly enriched with glycine (Supplemental Figure 7). Proteins with semirepetitive glycine-rich motifs are often named glycine-rich proteins (GRPs), which are a large group of proteins found in organisms ranging from bacteria to humans (Sachetto-Martins et al., 2000). Plant GRPs are diverse in terms of glycine domain organization, structure, function, subcellular localization, and expression pattern and modulation of their genes (Sachetto-Martins et al., 2000; Mangeon et al., 2010). Although the role of the glycine-rich domain present in the vast majority of GRPs remains obscure, it is widely believed that GRPs are part of multicomponent complexes where glycine-rich sequences are necessary for sustaining stability and conformational flexibility of protein-protein and protein-nucleic acid interactions (Sachetto-Martins et al., 2000; Mousavi and Hotta, 2005; Fusaro and Sachetto-Martins, 2007; Mangeon et al., 2010). Indeed, the glycine-rich motif of several bacterial and mammalian GRPs has been shown to be essential for physically associating with their interacting partners to form functional protein complexes (Lau et al., 1997; Suzuki et al., 1998; Friesen and Dreyfuss, 2000; Terasawa et al., 2006). In this study, we found that TGD5 physically interacts with TGD1, TGD2, TGD3, and TGD4. This result provides direct biochemical evidence that all five TGD proteins function as a single supercomplex in trafficking of the ER-derived lipids into chloroplasts. Further studies are needed to test the precise role of the glycine-rich domain of TGD5 in the formation and organization of the TGD supercomplex.

In the protease protection assays, TGD5 behaved like the inner envelope-localized TGD1 and TGD2 and was resistant to both thermolysin and trypsin. There are several possible reasons for the resistance of TGD5 to trypsin. First, TGD5 is deeply buried in the TGD complex and is protected by TGD1 and TGD2, the latter of which has at least eight copies per TGD1,2,3 complex (Roston et al., 2012). Second, the TGD complex is part of membrane contact sites between two envelopes and is inaccessible to trypsin. Third, TGD5 may be localized on the inside of the inner chloroplast envelope, but this location would be inconsistent with the results from Co-IP assays, which show that TGD5 physically interacts with the outer envelope protein TGD4. Further studies are needed to test these possibilities and the exact topology of TGD5.

Previous studies showed that TGD2 and TGD4 were present in two separate protein complexes residing in the outer and inner envelope of the chloroplast, respectively, and no additional proteins were found to be associated with either of these two complexes by mass spectrometry (Roston et al., 2012; Wang et al., 2012). This apparent discrepancy may be, at least in part, due to the technical difficulties in resolving the small mass proteins such as TGD5 (~9.2 kD) using single-percentage gels during PAGE. For example, the 10% SDS-PAGE gel used by Roston et al. (2012) may not be able to resolve TGD5, and in fact, their proteomic analysis focused on proteins with molecular masses larger than 20 kD. Another possibility is that TGD5 may interact transiently with

TGD2 and TGD4. Further studies are needed to determine the nature of the TGD interactions. Nevertheless, the dynamic interactions between TGD5 and other TGD proteins would be consistent with the transient nature of MCSs during leaf development (Whatley, 1974) and the temporal variations in the activity of ER-to-plastid lipid trafficking (Andersson et al., 2001).

The Increased Fatty Acid Synthesis May Explain the Pleiotropic Phenotypes in *tgd* Mutants

One of the diagnostic phenotypes for all *tgd* mutants is the accumulation of oligogalactolipids including TGDG due to the activation of a galactolipid:galactolipid galactosyltransferase (GGGT) (Xu et al., 2003, 2005). This enzyme is localized to the outer chloroplast envelope membrane (Xu et al., 2003) and catalyzes the processive transfer of the galactosyl residue of MGDG to various galactolipids, giving rise to oligogalactolipids and DAG. A recent study showed that GGGT is identical to SENSITIVE TO FREEZING2 (SFR2) (Moellering et al., 2010), but the exact mechanism leading to SFR2 activation in *tgd* mutants remains largely unknown. In vitro experiments showed that GGGT activity can be drastically stimulated by divalent cations (Heemskerk et al., 1987) and free fatty acids (FFAs) in the presence of limiting amounts of divalent cations (Sakaki et al., 1990b). Because fatty acid synthesis is markedly enhanced in both *tgd1-1* (Fan et al., 2013a) and *tgd5* mutants, and the majority of the de novo-synthesized fatty acids are exported into the cytosol to enter the β-oxidation pathway (Fan et al., 2013b), an attractive possibility is that GGGT is activated due to the passage of increased amounts of FFAs through the outer envelope membrane. In support of this, both oligogalactolipids and FFAs have also been reported to accumulate in isolated chloroplasts following prolonged incubation (Ongun and Mudd, 1968; Heemskerk et al., 1988) and in plants subjected to ozone fumigation (Sakaki et al., 1990a, 1990b).

Apart from oligogalactolipid accumulation, all five *tgd* mutants show changes in the fatty acid profile of membrane lipids with increased 18:1, particularly in PC (Xu et al., 2005, 2008; Awai et al., 2006; Lu et al., 2007; Supplemental Figure 3). Since 18:1 is the major fatty acid exported from the plastid (Ohlrogge and Jaworski, 1997), the majority of newly exported 18:1 is initially incorporated into PC through acyl editing (Bates et al., 2007, 2009), and PC is the major site of 18:1 desaturation in the ER (Sperling and Heinz, 1993), a marked increase in fatty acid synthesis in *tgd* mutants, and thus in 18:1 flux through PC, may overwhelm the ER fatty acid desaturation machinery, leading to an increase in 18:1 accumulation in PC. Similarly, the increased TAG accumulation is at least in part due to the increased rate of fatty acid synthesis, which outpaces the rate of TAG turnover through the peroxisomal β-oxidation pathway that is limited by SDP1 as shown in the *tgd1-1* mutant (Fan et al., 2014). Therefore, the majority of lipid phenotypes observed in *tgd* mutants likely result from the markedly increased fatty acid synthesis. Further studies are needed to understand how fatty acid synthesis is regulated in *tgd* mutants.

Biotechnological Implications for TGD5

Engineering oil accumulation in plant vegetative tissues has gained much interest as a potential platform for expanded production of oils as feed and as a source of renewable energy feedstock (Chapman et al., 2013; Troncoso-Ponce et al., 2013). One approach to enhancing TAG accumulation in vegetative tissues is the combined disruption of TGD1 and SDP1 (Fan et al., 2014). The rationale behind this approach is based on the observations that (1) the *tgd1* mutant shows a 4-fold increase in the rate of fatty acid synthesis in leaves (Fan et al., 2013a); (2) the increased fatty acid synthesis largely compensates for the defect in the eukaryotic lipid pathway so that the overall membrane lipid composition and plant growth remain largely unchanged (Xu et al., 2003); and (3) TAG is a key intermediate in fatty acid breakdown (Fan et al., 2014). Here, we show that knockout of TGD5 also results in marked increases in the rates of fatty acid synthesis and turnover and blocking TAG turnover by disrupting SDP1 in *tgd5-3* boosts leaf TAG accumulation to a level comparable to that observed in *tgd1-1 sdp1-4* (Fan et al., 2014). Importantly, unlike TGD1, which is essential for embryo development (Xu et al., 2005), knockout of TGD5 does not substantially affect seed development and has a less pronounced impact on plant vegetative growth than disruption of TGD1. Thus, *TGD5* offers a novel target for genetic engineering strategies aimed at exploring the feasibility of using abundant plant green biomass as nutrition-rich feed and a bioenergy feedstock.

METHODS

Plant Materials and Growth Conditions

The *Arabidopsis thaliana* plants used in this study were of the Columbia ecotype (Col-2). The *tgd1* mutant was previously described by Xu et al. (2003), *tgd2-1* by Awai et al. (2006), *tgd4-3* by Xu et al. (2008), *ats1-1* by Kunst et al. (1988), and *fad6* by Browse et al. (1989). The SAIL-T-DNA insertion mutants were isolated from the ABRC at Ohio State University (Alonso et al., 2003). The homozygosity of the T-DNA lines was verified using PCR primers specific for gene sequences: 5′-GCTAGTTGCTATGGGATG-3′ and 5′-CGGGTTTCATTGAGCAATC-3′ and the T-DNA left border primer 5′-GCGTGGACCGCTTGCTGCAAC-3′.

For growth on plates, surface-sterilized seeds of Arabidopsis were germinated on 0.6% (w/v) agar-solidified half-strength Murashige and Skoog (MS) (Murashige and Skoog, 1962) medium supplemented with 1% (w/v) sucrose in an incubator with a photon flux density of 80 to 120 μmol m^{-2} s^{-1} and a light period of 16 h (22°C) and a dark period of 8 h (18°C). For growth in soil, plants were first grown on MS medium for 10 d and then transferred to soil and grown under a photosynthetic photon flux density of 150 to 200 μmol m^{-2} s^{-1} at 22/18°C (day/night) with a 16-h-light/8-h-dark period.

Isolation of *TGD5* and Complementation Analysis

Approximately 40,000 Arabidopsis *fad6* seeds were mutagenized with ethyl methanesulfonate using standard procedures as previously described (Xu et al., 2003) and grown in 35 pools. M2 plants were grown under continuous light at 22°C for 3 weeks, and single leaves from individual M2 plants with pale-green appearance were used for determining the fatty acid composition by gas-liquid chromatography to identify mutants with increases in monounsaturated 18:1. The *tgd5-1* mutant was backcrossed to Col-2, and the progeny were analyzed for heritability of the pale-green phenotype and changes in fatty acid composition.

For positional cloning, the *tgd5-1* mutant was crossed with the wild-type plants of the Landsberg *erecta* ecotype, and 700 mutant plants were chosen from the F2 mapping population based on the presence of TGDG.

Simple sequence length polymorphism markers and cleaved amplified polymorphism sequence markers were designed based on the sequence polymorphism between Col and Landsberg *erecta* ecotypes and used to score the recombination events (Jander et al., 2002).

The full-length coding sequence of *TGD5* was amplified by RT-PCR from total RNA preparations using the primers 5′-ACCAGAGCTCATGGTGCTCTCTGACTTCAC-3′ and 5′-CACAGGTACCAGTGGAGTTTTTGGACATGT-3′. The PCR product was cloned into a binary vector pPZP212 (Hajdukiewicz et al., 1994) with GFP fused to the C terminus of TGD5. After confirming the integrity of the constructs by sequencing, plant stable transformation was performed according to Clough and Bent (1998). Genotyping at the *tgd5-1* locus was performed using a cleaved amplified polymorphism DNA marker with the PCR primers 5′-TCCGTTGCTTTCATGCA-3′ and 5′-CTCTAACTCGATGCCTTG-3′, since the point mutation in *tgd5-1* disrupts an *Hph*I digestion site in *TGD5*.

Bioinformatic Analysis of TGD5

Full-length deduced amino acid sequences were aligned using ClustalW (http://www.genome.jp/tools/clustalw/) and shaded using Boxshade (http://www.ch.embnet.org/software/BOX_form.html). The TMHMM program (Krogh et al., 2001) was used to predict the transmembrane domains shown in Supplemental Figure 7. For prediction of subcellular localization, we used data in the Arabidopsis subcellular database (SUBA; Heazlewood et al., 2007).

Co-IP and Immunoblotting

To generate constructs for Co-IP experiments, the full-length *TGD1* and *TGD2* genes were amplified with primers 5′-CACGGTACCATGATGCAGACTTGTTGT-3′ and 5′-CACGTCGACAACACAGTTCTTCAAAGA-3′ for *TGD1* and 5′-ACTTGAGCTCATGATTGGGAATCCAGTAAT-3′ and 5′-GATGGTACCTAGTAGCCTGCTTAGGGA-3′ for *TGD2*. To generate the DGD1N-HA construct, the *DGD1* cDNA sequence encoding the N-terminal portion of DGD1 up to Pro-337 (DGD1N) was amplified with forward primer 5′-CACGGTACCATGGTAAAGGAAACTCTA-3′ and reverse primer 5′-CACGTCGACAGGCTTCACAAAATCAGT-3′. The PCR products were cloned into the binary vector pPZP212 with a triple HA tag fused to the C termini of TGD1, TGD2, and DGD1N. The HA-TGD4 construct was previously described by Wang et al. (2012). To generate the TGD3-HA construct, the full-length *TGD3* gene was amplified with primers 5′-GTGGGGACAAGTTTGTACAAAAAAGCAGGCTTCATGCTTTCGTTATCATGCTC-3′ and 5′-GTGGGGACCACTTTGTACAAGAAAGCTGGGTCGTATCTGATTGGTCCATC-3′, and the PCR product was cloned into the Gateway binary vector pGWB414. For Co-IP assays, *Agrobacterium tumefaciens* cells carrying TGD5-GFP were coinfiltrated into tobacco leaves with constructs expressing TGD1-HA, TGD2-HA, TGD3-HA, HA-TGD4, or DGD1N-HA. Intact chloroplasts were isolated from the infiltrated leaves 3 d after infiltration as previously described (Xu et al., 2005), and isolated chloroplasts (10 μg chlorophyll) were then dissolved in 50 mM HEPES-KOH, pH 7.0, 150 mM NaCl, 1% dodecylmaltoside, and one protease inhibitor cocktail tablet (Roche) at 4°C for 30 min. Following centrifugation at 18,000*g* at 4°C for 30 min, the supernatant was incubated with Red Anti-HA Affinity gel beads (Sigma-Aldrich) overnight at 4°C with gentle shaking. The affinity beads were recovered by centrifugation at 1000*g* for 1 min and washed three times with washing buffer (50 mM HEPES-KOH, pH 7.0, 150 mM NaCl, 0.5% dodecylmaltoside, and one protease inhibitor cocktail tablet). The immunoprecipitates were then eluted by boiling with 2× SDS-PAGE sample buffer. Total proteins were extracted from the infiltrated tobacco leaves in 50 mM Tris-HCl, pH 8, 5% SDS, 10 mM DTT, 25 mM EDTA, and 0.1% phenylmethylsulfonyl fluoride. Cell debris was removed by centrifugation for 15 min (4°C, 14,000*g*). The total protein extracts (20 μg proteins) and the immunoprecipitates were separated by SDS-PAGE and immunoblot analysis was performed according to the procedures as previously described (Awai et al., 2006). The signals were visualized using an enhanced chemiluminescence detection kit (Thermal Scientific Pierce) or an alkaline phosphatase-conjugated system (Invitrogen).

Protease Protection Assay

To generate constructs for protease protection assays, the full-length *TGD1*, *OEP7*, and *ATS1* genes were amplified with primers 5′-GTGGGGACAAGTTTGTACAAAAAAGCAGGCTTCATGATGCAGACTTGTTGTAT-3′ and 5′-GTGGGGACCACTTTGTACAAGAAAGCTGGGTCAACACAGTTCTTCAAAGAATC-3′ for *TGD1*, 5′-GGTACCATGGGAAAAACTTCGGGAGC-3′ and 5′-TCTAGACAAACCCTCTTTGGATGTGG-3′ for *OEP7*, and 5′-GTGGGGACAAGTTTGTACAAAAAAGCAGGCTTCATGACTCTCACGTTTTCCTCC-3′ and 5′-GTGGGGACCACTTTGTACAAGAAAGCTGGGTCATTCCAAGGTTGTGACAAAGAGA-3′ for *ATS1*. The *TGD1* and *ATS1* PCR products were then cloned into the Gateway binary vector pGWB414. The *OEP7* PCR product was cloned into the binary vector pPZP212 with a GFP fused to the C terminus of OEP7. Agrobacterium strains carrying TGD5-GFP, TGD2-HA, TGD1-HA, OEP7-GFP, or HA-TGD4 were transiently expressed in tobacco leaves as described above. At 3 d after infiltration, intact chloroplasts were isolated by discontinuous Percoll gradient as previously described (Xu et al., 2005). Protease protection experiments were performed according to McAndrew et al. (2001). Briefly, isolated chloroplasts were treated with either trypsin or thermolysin at final concentrations of 500 or 800 μg/mL for 30 min in ice-cold reaction buffer (50 mM HEPES-KOH, pH 7.9, 0.33 M sorbitol, and 1 mM $CaCl_2$) in a total volume of 100 μL. After termination of the digestion by addition of an equal volume of quenching buffer (50 mM HEPES-KOH, pH 7.9, 0.33 M sorbitol, 10 mM EDTA, and one protease inhibitor cocktail tablet). The protease-treated intact chloroplasts were reisolated by centrifugation (5000*g* at 4°C for 5 min) through 40% Percoll (v/v), washed once with quenching buffer, and solubilized directly in sample buffer prior to SDS-PAGE and immunoblot analyses.

Subfractionation of Chloroplasts

Intact chloroplasts (20 mg of chlorophyll) isolated from 4-week-old transgenic plants overexpressing TGD5-GFP were fractionated into thylakoids and envelope membranes according to Cline et al. (1981). Total proteins were extracted from leaves of 4-week-old plants as described above. Equal amounts of proteins were used for SDS-PAGE and immunoblot analysis.

RNA Extraction and RT-PCR Analysis

Total RNA was extracted using TRIzol reagent. SuperScript II reverse transcriptase (Invitrogen) was used for first-strand cDNA synthesis. TGD5 expression was detected using primers P1 (5′-ATGGTGCTCTCTGACTTCAC-3′), P2 (5′-TTAAGTGGAGTTTTTGGAC-3′), and P3 (5′-CTCTAACTCGATGCCTTG-3′). The internal standard *UBQ10* was amplified using forward primer 5′-TCAATTCTCTCTACCGTGATCAAGATGCA-3′ and reverse primer 5′-GGTGTCAGAACTCTCCACCTCAAGAGTA-3′.

Lipid and Fatty Acid Analyses

Total lipids were extracted by homogenization in chloroform/methanol/formic acid (1:2:0.1, by volume) and 1 M KCl-0.2 M H_3PO_4 according to Dörmann et al. (1995). Neutral and total polar lipids were separated on silica plates (Si250 with preadsorbant layer; Mallinckrodt Baker) by TLC as described (Fan et al., 2013a). After TLC, individual lipids were scraped from the plate and used to prepare fatty acid methyl esters (FAMEs) by acid-catalyzed transmethylation. To quantify the total leaf fatty acid content, total lipid extracts were transmethylated into FAMEs directly. FAMEs were separated and quantified as described (Fan et al., 2011). Oligogalactolipids

and TAG on TLC plates were visualized by spraying 5% H_2SO_4 followed by charring. The fatty acid composition at the *sn-2* position of the glycerol backbone was determined by *Rhizopus arrhizus* lipase digestion as described by Härtel et al. (2000).

Acetate Labeling

In vivo labeling experiments with ^{14}C-acetate were done according to Koo et al. (2005). Briefly, rapidly growing leaves of 7-week-old plants were cut in strips and then incubated in the light (60 μmol m^{-2} s^{-1} at 22°C with shaking in 10 mL of medium containing 1 mM unlabeled acetate, 20 mM MES pH 5.5, one-tenth strength of MS salts, and 0.01% Tween 20). The assay was started by the addition of 0.1 mCi of ^{14}C-acetate (106 mCi/mmol; American Radiolabeled Chemicals). At the end of incubation, leaf strips were washed three times with water and blotted onto filter paper. For the chase period, leaf tissue was incubated in the same medium lacking ^{14}C-acetate as used for the pulse. Total lipids were extracted and separated as described above and radioactivity associated with total lipids or different lipid classes was determined by liquid scintillation counting.

Microscopy

Siliques were imaged using a Leica dissecting microscope (Leica Microsystems) equipped with a Spot Insight color camera. Developing seeds were cleared in chloral hydrate solution (chloral hydrate:water:glycerol, 8:2:1 w/v/v) overnight at 4°C and were observed with a Zeiss epifluorescence microscope (Carl Zeiss Axiovert 200M). In vivo pollen germination assays were done as described (Fan et al., 2014).

For lipid droplet imaging, leaf tissues were stained with a neutral lipid-specific fluorescent dye, Nile red (Sigma-Aldrich), at a final concentration of 10 μg/mL and observed under a Zeiss epifluorescence microscope (Carl Zeiss; Axiovert 200M) with a GFP filter.

For the TGD5-GFP fusion protein localization study, leaf samples were mounted in water on slides and directly examined using a Leica TCS SP5 confocal scanning laser microscope with excitation at 488 nm and emission at 505 to 550 nm for GFP fluorescence and 636 to 750 nm for chlorophyll autofluorescence. For transmission electron microscopy, leaf tissues were fixed with 2.5% (v/v) glutaraldehyde in 0.1 M sodium cacodylate buffer (pH 7.4) for 2 h and then postfixed with 1% osmium tetroxide in the same buffer for 2 h at room temperature. After dehydration in a graded series of ethanol, the tissues were embedded in EPON812 resin (Electron Microscopy Sciences), sectioned, and stained with 2% uranyl acetate and lead citrate before viewing under a Jeol JEM-1400 LaB6 120-keV transmission electron microscope.

Accession Numbers

Sequence data from this article can be found in the Arabidopsis Genome Initiative or GenBank/EMBL database under the following accession numbers: *ATS1*, At1g32200; *DGD1*, At3g11670; *OEP7*, At3g52420; *TGD1*, At1g19800; *TGD2*, At3g20320; *TGD3*, At1g65410; *TGD4*, AT3g06960; *TGD5*, At1g27695; and *SDP1*, At5g04040.

Supplemental Data

Supplemental Figure 1. Growth and Lipid Phenotypes of the *tgd5 fad6* Double Mutant.

Supplemental Figure 2. Complementation of the *tgd5-1* Mutation by the *TGD5* cDNA Fused at the C Terminus with GFP.

Supplemental Figure 3. Fatty Acid Composition of Major Membrane Lipids in Leaves of *tgd5* Mutants.

Supplemental Figure 4. Fatty Acid Composition of Leaf TAG.

Supplemental Figure 5. The Pollen Grain Germination Defect of *tgd4-3 tgd5-3* Double Mutant.

Supplemental Figure 6. Fatty Acid Composition of Major Membrane Lipids in Leaves of *tgd4-3* and *tgd5-3* Single and *tgd4-3 tgd5-3* Double Mutants.

Supplemental Figure 7. Comparison of the Predicted Arabidopsis TGD5 Protein and Its Homologs in Different Plant Species.

ACKNOWLEDGMENTS

We thank Christoph Benning for kindly allowing us to initiate the genetic mutant screen in his lab and for providing *tgd1-1*, *tgd2-1*, and *tgd4-3* mutant seeds. We thank John Shanklin for critical reading of the article. This material is based upon work supported by the U.S. Department of Energy, Office of Science, Office of Basic Energy Sciences, Chemical Sciences, Geosciences, and Biosciences Division under Contract DEAC0298CH10886. Use of the transmission electron microscope and the confocal microscope at the Center of Functional Nanomaterials was supported by the Office of Basic Energy Sciences, U.S. Department of Energy, under Contract DE-SC0012704.

AUTHOR CONTRIBUTIONS

C.X. and J.F. designed the experiments, participated in data analysis, and wrote the article. J.F., C.Y., Z.Z., and C.X. performed the research.

Received May 4, 2015; revised August 24, 2015; accepted September 4, 2015; published September 28, 2015.

REFERENCES

Alonso, J.M., et al. (2003). Genome-wide insertional mutagenesis of *Arabidopsis thaliana.* Science **301:** 653–657.

Andersson, M.X., Kjellberg, J.M., and Sandelius, A.S. (2001). Chloroplast biogenesis. Regulation of lipid transport to the thylakoid in chloroplasts isolated from expanding and fully expanded leaves of pea. Plant Physiol. **127:** 184–193.

Awai, K., Maréchal, E., Block, M.A., Brun, D., Masuda, T., Shimada, H., Takamiya, K., Ohta, H., and Joyard, J. (2001). Two types of MGDG synthase genes, found widely in both 16:3 and 18:3 plants, differentially mediate galactolipid syntheses in photosynthetic and nonphotosynthetic tissues in *Arabidopsis thaliana.* Proc. Natl. Acad. Sci. USA **98:** 10960–10965.

Awai, K., Xu, C., Tamot, B., and Benning, C. (2006). A phosphatidic acid-binding protein of the chloroplast inner envelope membrane involved in lipid trafficking. Proc. Natl. Acad. Sci. USA **103:** 10817–10822.

Bates, P.D., Durrett, T.P., Ohlrogge, J.B., and Pollard, M. (2009). Analysis of acyl fluxes through multiple pathways of triacylglycerol synthesis in developing soybean embryos. Plant Physiol. **150:** 55–72.

Bates, P.D., Ohlrogge, J.B., and Pollard, M. (2007). Incorporation of newly synthesized fatty acids into cytosolic glycerolipids in pea leaves occurs via acyl editing. J. Biol. Chem. **282:** 31206–31216.

Benning, C. (2007). Questions remaining in sulfolipid biosynthesis: a historical perspective. Photosynth. Res. **92:** 199–203.

Benning, C. (2009). Mechanisms of lipid transport involved in organelle biogenesis in plant cells. Annu. Rev. Cell Dev. Biol. **25:** 71–91.

Browse, J., and Somerville, C. (1991). Glycerolipid synthesis - Biochemistry and regulation. Annu. Rev. Plant Physiol. Plant Mol. Biol. **42:** 467–506.

Browse, J., Kunst, L., Anderson, S., Hugly, S., and Somerville, C. (1989). A mutant of Arabidopsis deficient in the chloroplast 16:1/18:1 desaturase. Plant Physiol. **90:** 522–529.

Carde, J.P., Joyard, J., and Douce, R. (1982). Electron-microscopic studies of envelope membranes from spinach plastids. Biol. Cell **44:** 315.

Chapman, K.D., Dyer, J.M., and Mullen, R.T. (2013). Commentary: why don't plant leaves get fat? Plant Sci. **207:** 128–134.

Chng, S.S., Gronenberg, L.S., and Kahne, D. (2010). Proteins required for lipopolysaccharide assembly in *Escherichia coli* form a transenvelope complex. Biochemistry **49:** 4565–4567.

Cline, K., Andrews, J., Mersey, B., Newcomb, E.H., and Keegstra, K. (1981). Separation and characterization of inner and outer envelope membranes of pea chloroplasts. Proc. Natl. Acad. Sci. USA **78:** 3595–3599.

Clough, S.J., and Bent, A.F. (1998). Floral dip: a simplified method for Agrobacterium-mediated transformation of *Arabidopsis thaliana.* Plant J. **16:** 735–743.

Cremers, F.F.M., Voorhout, W.F., Vanderkrift, T.P., Leunissenbijvelt, J.J.M., and Verkleij, A.J. (1988). Visualization of contact sites between outer and inner envelope membranes in isolated chloroplasts. Biochim. Biophys. Acta **933:** 334–340.

Dörmann, P., Balbo, I., and Benning, C. (1999). Arabidopsis galactolipid biosynthesis and lipid trafficking mediated by DGD1. Science **284:** 2181–2184.

Dörmann, P., Hoffmann-Benning, S., Balbo, I., and Benning, C. (1995). Isolation and characterization of an Arabidopsis mutant deficient in the thylakoid lipid digalactosyl diacylglycerol. Plant Cell **7:** 1801–1810.

Eastmond, P.J. (2006). SUGAR-DEPENDENT1 encodes a patatin domain triacylglycerol lipase that initiates storage oil breakdown in germinating Arabidopsis seeds. Plant Cell **18:** 665–675.

Elbaz, Y., and Schuldiner, M. (2011). Staying in touch: the molecular era of organelle contact sites. Trends Biochem. Sci. **36:** 616–623.

Fan, J., Andre, C., and Xu, C. (2011). A chloroplast pathway for the de novo biosynthesis of triacylglycerol in *Chlamydomonas reinhardtii.* FEBS Lett. **585:** 1985–1991.

Fan, J., and Xu, C. (2011). Genetic analysis of Arabidopsis mutants impaired in plastid lipid import reveals a role of membrane lipids in chloroplast division. Plant Signal. Behav. **6:** 458–460.

Fan, J., Yan, C., Roston, R., Shanklin, J., and Xu, C. (2014). Arabidopsis lipins, PDAT1 acyltransferase, and SDP1 triacylglycerol lipase synergistically direct fatty acids toward β-oxidation, thereby maintaining membrane lipid homeostasis. Plant Cell **26:** 4119–4134.

Fan, J., Yan, C., and Xu, C. (2013a). Phospholipid:diacylglycerol acyltransferase-mediated triacylglycerol biosynthesis is crucial for protection against fatty acid-induced cell death in growing tissues of Arabidopsis. Plant J. **76:** 930–942.

Fan, J., Yan, C., Zhang, X., and Xu, C. (2013b). Dual role for phospholipid:diacylglycerol acyltransferase: enhancing fatty acid synthesis and diverting fatty acids from membrane lipids to triacylglycerol in Arabidopsis leaves. Plant Cell **25:** 3506–3518.

Friesen, W.J., and Dreyfuss, G. (2000). Specific sequences of the Sm and Sm-like (Lsm) proteins mediate their interaction with the spinal muscular atrophy disease gene product (SMN). J. Biol. Chem. **275:** 26370–26375.

Froehlich, J.E., Benning, C., and Dörmann, P. (2001). The digalactosyldiacylglycerol (DGDG) synthase DGD1 is inserted into the outer envelope membrane of chloroplasts in a manner independent of the general import pathway and does not depend on direct interaction with monogalactosyldiacylglycerol synthase for DGDG biosynthesis. J. Biol. Chem. **276:** 31806–31812.

Fusaro, A.F., and Sachetto-Martins, G. (2007). Blooming time for plant glycine-rich proteins. Plant Signal. Behav. **2:** 386–387.

Hajdukiewicz, P., Svab, Z., and Maliga, P. (1994). The small, versatile pPZP family of Agrobacterium binary vectors for plant transformation. Plant Mol. Biol. **25:** 989–994.

Härtel, H., Dormann, P., and Benning, C. (2000). DGD1-independent biosynthesis of extraplastidic galactolipids after phosphate deprivation in Arabidopsis. Proc. Natl. Acad. Sci. USA **97:** 10649–10654.

Heazlewood, J.L., Verboom, R.E., Tonti-Filippini, J., Small, I., and Millar, A.H. (2007). SUBA: the Arabidopsis Subcellular Database. Nucleic Acids Res. **35:** D213–D218.

Heemskerk, J.W.M., Bogemann, G., Helsper, J.P.F.G., and Wintermans, J.F.G.M. (1988). Synthesis of monogalactosyldiacylglycerol and digalactosyldiacylglycerol in isolated spinach chloroplasts. Plant Physiol. **86:** 971–977.

Heemskerk, J.W.M., Jacobs, F.H.H., Scheijen, M.A.M., Helsper, J.P.F.G., and Wintermans, J.F.G.M. (1987). Characterization of galactosyltransferases in spinach chloroplast envelopes. Biochim. Biophys. Acta **918:** 189–203.

Helle, S.C., Kanfer, G., Kolar, K., Lang, A., Michel, A.H., and Kornmann, B. (2013). Organization and function of membrane contact sites. Biochim. Biophys. Acta **1833:** 2526–2541.

Hurlock, A.K., Roston, R.L., Wang, K., and Benning, C. (2014). Lipid trafficking in plant cells. Traffic **15:** 915–932.

Jander, G., Norris, S.R., Rounsley, S.D., Bush, D.F., Levin, I.M., and Last, R.L. (2002). Arabidopsis map-based cloning in the post-genome era. Plant Physiol. **129:** 440–450.

Jessen, D., Roth, C., Wiermer, M., and Fulda, M. (2015). Two activities of long-chain acyl-coenzyme A synthetase are involved in lipid trafficking between the endoplasmic reticulum and the plastid in Arabidopsis. Plant Physiol. **167:** 351–366.

Koo, A.J.K., Fulda, M., Browse, J., and Ohlrogge, J.B. (2005). Identification of a plastid acyl-acyl carrier protein synthetase in Arabidopsis and its role in the activation and elongation of exogenous fatty acids. Plant J. **44:** 620–632.

Krogh, A., Larsson, B., von Heijne, G., and Sonnhammer, E.L. (2001). Predicting transmembrane protein topology with a hidden Markov model: application to complete genomes. J. Mol. Biol. **305:** 567–580.

Kunst, L., Browse, J., and Somerville, C. (1988). Altered regulation of lipid biosynthesis in a mutant of Arabidopsis deficient in chloroplast glycerol-3-phosphate acyltransferase activity. Proc. Natl. Acad. Sci. USA **85:** 4143–4147.

Lau, P.P., Zhu, H.J., Nakamuta, M., and Chan, L. (1997). Cloning of an Apobec-1-binding protein that also interacts with apolipoprotein B mRNA and evidence for its involvement in RNA editing. J. Biol. Chem. **272:** 1452–1455.

Lev, S. (2010). Non-vesicular lipid transport by lipid-transfer proteins and beyond. Nat. Rev. Mol. Cell Biol. **11:** 739–750.

Lu, B., Xu, C., Awai, K., Jones, A.D., and Benning, C. (2007). A small ATPase protein of Arabidopsis, TGD3, involved in chloroplast lipid import. J. Biol. Chem. **282:** 35945–35953.

Malinverni, J.C., and Silhavy, T.J. (2009). An ABC transport system that maintains lipid asymmetry in the gram-negative outer membrane. Proc. Natl. Acad. Sci. USA **106:** 8009–8014.

Mangeon, A., Junqueira, R.M., and Sachetto-Martins, G. (2010). Functional diversity of the plant glycine-rich proteins superfamily. Plant Signal. Behav. **5:** 99–104.

McAndrew, R.S., Froehlich, J.E., Vitha, S., Stokes, K.D., and Osteryoung, K.W. (2001). Colocalization of plastid division proteins in the chloroplast stromal compartment establishes a new functional relationship between FtsZ1 and FtsZ2 in higher plants. Plant Physiol. **127:** 1656–1666.

McConn, M., and Browse, J. (1998). Polyunsaturated membranes are required for photosynthetic competence in a mutant of Arabidopsis. Plant J. **15:** 521–530.

Mehrshahi, P., Stefano, G., Andaloro, J.M., Brandizzi, F., Froehlich, J.E., and DellaPenna, D. (2013). Transorganellar complementation redefines the biochemical continuity of endoplasmic reticulum and chloroplasts. Proc. Natl. Acad. Sci. USA **110:** 12126–12131.

Moellering, E.R., Muthan, B., and Benning, C. (2010). Freezing tolerance in plants requires lipid remodeling at the outer chloroplast membrane. Science **330:** 226–228.

Mongrand, S., Cassagne, C., and Bessoule, J.J. (2000). Import of lyso-phosphatidylcholine into chloroplasts likely at the origin of eukaryotic plastidial lipids. Plant Physiol. **122:** 845–852.

Mousavi, A., and Hotta, Y. (2005). Glycine-rich proteins: a class of novel proteins. Appl. Biochem. Biotechnol. **120:** 169–174.

Murashige, T., and Skoog, F. (1962). A revised medium for rapid growth and bio assays with tobacco tissue cultures. Physiol. Plant. **15:** 473–497.

Nakamura, Y., Andrés, F., Kanehara, K., Liu, Y.C., Dörmann, P., and Coupland, G. (2014). Arabidopsis florigen FT binds to diurnally oscillating phospholipids that accelerate flowering. Nat. Commun. **5:** 3553.

Ohlrogge, J., and Browse, J. (1995). Lipid biosynthesis. Plant Cell **7:** 957–970.

Ohlrogge, J.B., and Jaworski, J.G. (1997). Regulation of fatty acid synthesis. Annu. Rev. Plant Physiol. Plant Mol. Biol. **48:** 109–136.

Ongun, A., and Mudd, J.B. (1968). Biosynthesis of galactolipids in plants. J. Biol. Chem. **243:** 1558–1566.

Paila, Y.D., Richardson, L.G., and Schnell, D.J. (2015). New insights into the mechanism of chloroplast protein import and its integration with protein quality control, organelle biogenesis and development. J. Mol. Biol. **427:** 1038–1060.

Roston, R., Gao, J., Xu, C., and Benning, C. (2011). Arabidopsis chloroplast lipid transport protein TGD2 disrupts membranes and is part of a large complex. Plant J. **66:** 759–769.

Roston, R.L., Gao, J., Murcha, M.W., Whelan, J., and Benning, C. (2012). TGD1, -2, and -3 proteins involved in lipid trafficking form ATP-binding cassette (ABC) transporter with multiple substrate-binding proteins. J. Biol. Chem. **287:** 21406–21415.

Roughan, P.G., and Slack, C.R. (1982). Cellular organization of glycerolipid metabolism. Annu. Rev. Plant Physiol. **33:** 97–132.

Sachetto-Martins, G., Franco, L.O., and de Oliveira, D.E. (2000). Plant glycine-rich proteins: a family or just proteins with a common motif? Biochim. Biophys. Acta **1492:** 1–14.

Sakaki, T., Kondo, N., and Yamada, M. (1990a). Pathway for the synthesis of triacylglycerols from monogalactosyldiacylglycerols in ozone-fumigated spinach leaves. Plant Physiol. **94:** 773–780.

Sakaki, T., Saito, K., Kawaguchi, A., Kondo, N., and Yamada, M. (1990b). Conversion of monogalactosyldiacylglycerols to triacylglycerols in ozone-fumigated spinach leaves. Plant Physiol. **94:** 766–772.

Schleiff, E., Tien, R., Salomon, M., and Soll, J. (2001). Lipid composition of outer leaflet of chloroplast outer envelope determines topology of OEP7. Mol. Biol. Cell **12:** 4090–4102.

Sessions, A., et al. (2002). A high-throughput Arabidopsis reverse genetics system. Plant Cell **14:** 2985–2994.

Soll, J., and Schleiff, E. (2004). Protein import into chloroplasts. Nat. Rev. Mol. Cell Biol. **5:** 198–208.

Sperandeo, P., Lau, F.K., Carpentieri, A., De Castro, C., Molinaro, A., Dehò, G., Silhavy, T.J., and Polissi, A. (2008). Functional analysis of the protein machinery required for transport of lipopolysaccharide to the outer membrane of *Escherichia coli.* J. Bacteriol. **190:** 4460–4469.

Sperling, P., and Heinz, E. (1993). Isomeric *sn*-1-octadecenyl and *sn*-2-octadecenyl analogues of lysophosphatidylcholine as substrates for acylation and desaturation by plant microsomal membranes. Eur. J. Biochem. **213:** 965–971.

Suzuki, T., Miki, H., Takenawa, T., and Sasakawa, C. (1998). Neural Wiskott-Aldrich syndrome protein is implicated in the actin-based motility of *Shigella flexneri.* EMBO J. **17:** 2767–2776.

Symmons, M.F., Bokma, E., Koronakis, E., Hughes, C., and Koronakis, V. (2009). The assembled structure of a complete tripartite bacterial multidrug efflux pump. Proc. Natl. Acad. Sci. USA **106:** 7173–7178.

Tanaka, T., Ohnishi, J., and Yamada, M. (1980). The occurrence of phosphatidyl choline exchange protein in leaves. Biochem. Biophys. Res. Commun. **96:** 394–399.

Tatsuta, T., Scharwey, M., and Langer, T. (2014). Mitochondrial lipid trafficking. Trends Cell Biol. **24:** 44–52.

Terasawa, K., Yoshimatsu, K., Iemura, S., Natsume, T., Tanaka, K., and Minami, Y. (2006). Cdc37 interacts with the glycine-rich loop of Hsp90 client kinases. Mol. Cell. Biol. **26:** 3378–3389.

Troncoso-Ponce, M.A., Cao, X., Yang, Z., and Ohlrogge, J.B. (2013). Lipid turnover during senescence. Plant Sci. **205-206:** 13–19.

Wang, Z., Xu, C., and Benning, C. (2012). TGD4 involved in endoplasmic reticulum-to-chloroplast lipid trafficking is a phosphatidic acid binding protein. Plant J. **70:** 614–623.

Whatley, J.M. (1974). Chloroplast development in primary leaves of *Phaseolus vulgaris.* New Phytol. **71:** 1097–1110.

Williams, J.P., Imperial, V., Khan, M.U., and Hodson, J.N. (2000). The role of phosphatidylcholine in fatty acid exchange and desaturation in *Brassica napus* L. leaves. Biochem. J. **349:** 127–133.

Wu, G.Z., and Xue, H.W. (2010). Arabidopsis β-ketoacyl-[acyl carrier protein] synthase i is crucial for fatty acid synthesis and plays a role in chloroplast division and embryo development. Plant Cell **22:** 3726–3744.

Xu, C., Fan, J., Cornish, A.J., and Benning, C. (2008). Lipid trafficking between the endoplasmic reticulum and the plastid in Arabidopsis requires the extraplastidic TGD4 protein. Plant Cell **20:** 2190–2204.

Xu, C., Fan, J., Froehlich, J.E., Awai, K., and Benning, C. (2005). Mutation of the TGD1 chloroplast envelope protein affects phosphatidate metabolism in Arabidopsis. Plant Cell **17:** 3094–3110.

Xu, C., Fan, J., Riekhof, W., Froehlich, J.E., and Benning, C. (2003). A permease-like protein involved in ER to thylakoid lipid transfer in Arabidopsis. EMBO J. **22:** 2370–2379.

Xu, C., Moellering, E.R., Muthan, B., Fan, J., and Benning, C. (2010). Lipid transport mediated by Arabidopsis TGD proteins is unidirectional from the endoplasmic reticulum to the plastid. Plant Cell Physiol. **51:** 1019–1028.

Xu, C., Yu, B., Cornish, A.J., Froehlich, J.E., and Benning, C. (2006). Phosphatidylglycerol biosynthesis in chloroplasts of Arabidopsis mutants deficient in acyl-ACP glycerol-3-phosphate acyltransferase. Plant J. **47:** 296–309.